geosciences

MDPI

Article

The Granite Aqueduct and Autometamorphism of Plutons

John M. Bartley [1,*], Allen F. Glazner [2], Michael A. Stearns [3] and Drew S. Coleman [2]

[1] Department of Geology and Geophysics, University of Utah, Salt Lake City, UT 84112-0101, USA
[2] Department of Geological Sciences, University of North Carolina, Chapel Hill, North Carolina, NC 27599, USA; afg@unc.edu (A.F.G.); dcoleman@email.unc.edu (D.S.C.)
[3] Department of Earth Science, Utah Valley University, Orem, UT 84058, USA; mstearns@uvu.edu
* Correspondence: john.bartley@utah.edu

Received: 29 February 2020; Accepted: 8 April 2020; Published: 10 April 2020

Abstract: Ian Carmichael wrote of an "andesite aqueduct" that conveys vast amounts of water from the magma source region of a subduction zone to the Earth's surface. Diverse observations indicate that subduction zone magmas contain 5 wt % or more H_2O. Most of the water is released from crystallizing intrusions to play a central role in contact metamorphism and the genesis of ore deposits, but it also has important effects on the plutonic rocks themselves. Many plutons were constructed incrementally from the top down over million-year time scales. Early-formed increments are wall rocks to later increments; heat and water released as each increment crystallizes pass through older increments before exiting the pluton. The water ascends via multiple pathways. Hydrothermal veins record ascent via fracture conduits. Pipe-like conduits in Yosemite National Park, California, are located in or near aplite–pegmatite dikes, which themselves are products of hydrous late-stage magmatic liquids. Pervasive grain-boundary infiltration is recorded by fluid-mediated subsolidus modification of mineral compositions and textures. The flood of magmatic water carries a large fraction of the total thermal energy of the magma and transmits that energy much more rapidly than conduction, thus enhancing the fluctuating postemplacement thermal histories that result from incremental pluton growth. The effects of water released by subduction zone magmas are central not only to metamorphism and mineralization of surrounding rocks, but also to the petrology and the thermal history of the plutons themselves.

Keywords: incremental intrusion; hydrothermal fluid; microstructure; dissolution; precipitation; textural coarsening

1. Introduction

It has long been appreciated that water released by arc plutons plays a central role in the genesis of ore deposits as well as in contact metamorphism. Carmichael [1] used phase equilibria and thermodynamic arguments to estimate the water contents of volcanic arc magmas, and concluded that subduction-related intermediate magmas typically contain several percent water. He also estimated the plutonic/volcanic ratio in arcs to be approximately 5 and thus suggested that more than 80% of the water carried upward by arc magmas is released beneath the Earth's surface by crystallization of intrusive bodies. Although a small proportion of the water released by subsurface crystallization is fixed in hydrous minerals, most must be released to the surface at volcanic vents and via diffuse flow.

Effects of the prodigious amount of water carried by arc magmas on the plutonic rocks themselves have generally been underappreciated. Magma bodies solidify predominantly from the top down and from the outside in, and geochronology indicates that granitic plutons commonly grow incrementally by downward stacking of sheets (Figure 1; [2,3]). The majority of the water released by crystallizing

magma therefore must pass through already solidified plutonic rock by some combination of fracture flow, grain-boundary flow, and diffusion before it encounters wall rocks (Figure 2). In this paper, we argue that passage of this water promotes textural modification and re-equilibration of minerals to lower temperatures via dissolution–precipitation and net-transfer reactions, and that such postmagmatic modification is ubiquitous and a key element in understanding the textural development of granitic rocks and the assembly of granitic plutons.

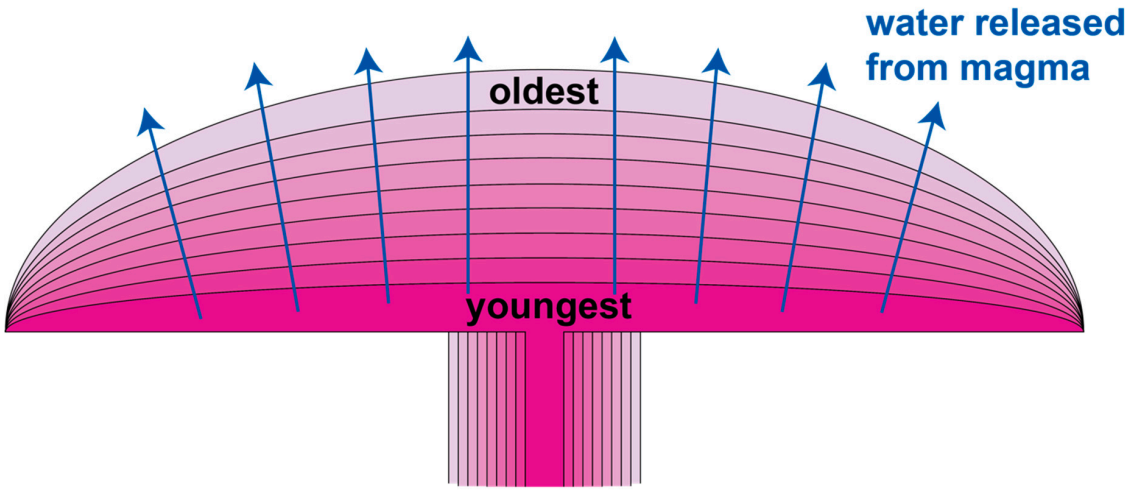

Figure 1. Schematic diagram illustrating incremental pluton growth by downward stacking of intrusive increments. Space for each increment is made by opening of a subhorizontal crack and accommodated by some combination of roof uplift and floor subsidence. Arrows represent migrating water released by crystallization. Buoyancy will cause much of the water to ascend through overlying older increments but migration paths will be strongly affected by the spatial pattern of permeability.

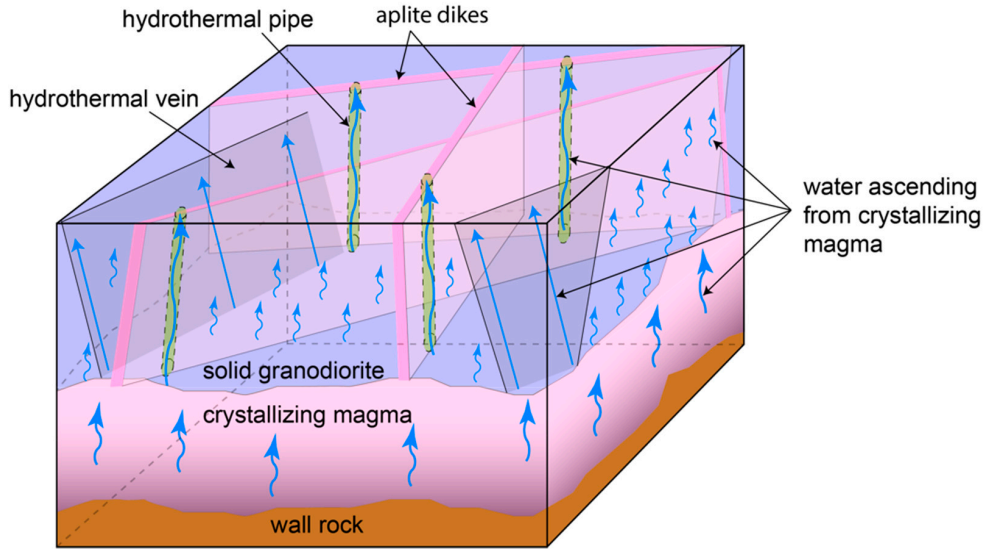

Figure 2. Schematic diagram illustrating fluid ascent paths in a growing pluton. The pluton is assumed to grow and to crystallize downward from its roof (not shown). Aplite dikes are fed by felsic melt that accumulates at the top of the active magma body [4,5].

2. Amount of Water in Arc Magmas and Arc Rocks

Several lines of evidence indicate that arc magmas typically contain several wt % H_2O. Sisson and Layne [6] reported water contents up to approximately 6 wt % in glass inclusions from mafic arc magmas. Measured water contents of 134 melt inclusions in arc rocks ranging from basalt to dacite [7] average 3.7 wt %; compilation for basalts and basaltic andesites averages somewhat less, around 2.5 wt % [8]. Plank

et al. [9] reported an average of about 4 wt % H_2O for mafic arc magmas. Water contents of inclusions do not directly measure the content in the magma owing to degassing before entrapment, crystallization after entrapment, and other phenomena, so these measurements are not definitive. Estimates based on phase equilibria (e.g., water contents needed to reproduce a given phase assemblage) lead to significantly higher estimated water contents of 6 wt % to greater than 8 wt % (e.g., [1,10,11]).

Water contents of rocks crystallized from arc magmas are significantly lower than the estimated magmatic compositions. Granites and granodiorites from the EarthChem database have median H_2O^+ contents of 0.6 wt % (Figure 3). Given the magma water contents above and these data, for the purposes of argument we assume that typical intermediate arc magmas release 5 wt % H_2O upon full crystallization.

Five wt % H_2O is a surprisingly large volume. If 1 kg of magma releases 5 wt % H_2O while crystallizing to a rock with density 2700 kg/m^3, the water, if condensed, has roughly 15% of the volume of the crystallized rock. Consider an end-member scenario of vertical ascent of 100% of the magmatic water released from crystallization of a 3 km thick stack of sheets emplaced in top-down fashion. Roughly 375,000 kg of magmatic H_2O per square meter must ascend through the roof of the pluton—enough to form a layer of condensed water 450 m thick. Cumulative water/rock ratio will decrease passing downward, but the substantial majority of the pluton nonetheless must have interacted with a large volume of water released from deeper magma.

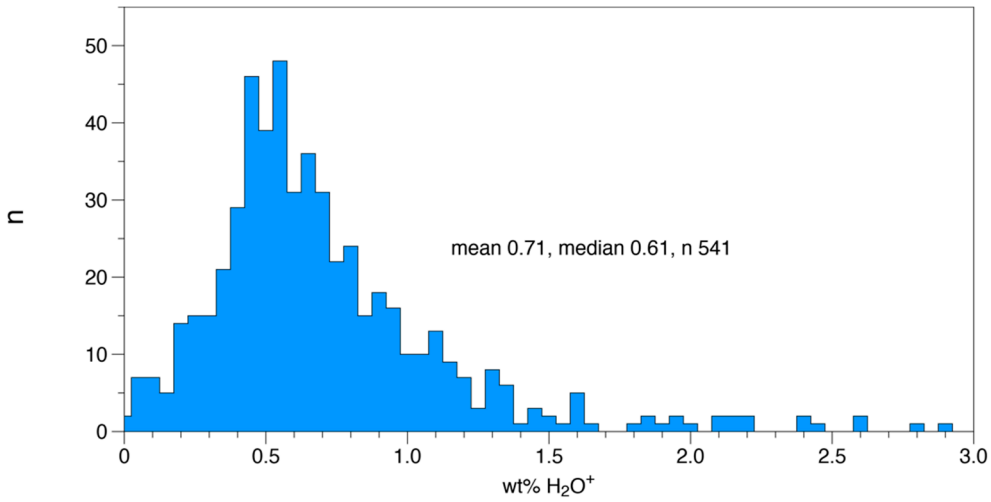

Figure 3. Weight percent H_2O^+ in rocks labeled as granite or granodiorite, with determinations by USGS rapid rock, wet chemistry, or gravimetry, in the EarthChem database.

3. Incremental Pluton Growth

It is now widely accepted that large plutons commonly grow incrementally over million-year time scales (e.g., [2,12,13]). The most compelling support for incremental growth comes from geochronological results that record growth durations far longer than durations indicated by thermal modeling of plutons emplaced as single magma bodies (e.g., [14,15]). Field evidence from some plutons corroborates incremental growth. Plutons that grew by magmatic crack-seal [16] can contain arrays of wall-rock inclusions that are concordant with wall-rock structure adjacent to the pluton (e.g., [14,17,18]). The Half Dome Granodiorite of the Tuolumne Intrusive Suite in Yosemite National Park, California, contains km-scale cyclical variations in composition that are interpreted to record episodic freezing owing to waning of the magma flux during incremental growth [4]. Incremental growth of the felsic parts of Half Dome compositional cycles is indicated by multiple generations of crosscutting dikes that range in composition from granodiorite to leucogranite [5].

4. Downward Growth of Plutons

Spatial patterns of U-Pb zircon dates in the Tuolumne Intrusive Suite [2] and field and geochronologic evidence from other examples (e.g., [19–23]) indicate that large plutons commonly grow by downward stacking of intrusive sheets. In the Tuolumne Intrusive Suite, this pattern applies both to the relations between major map units (Kuna Crest, Half Dome, Cathedral Peak) and to the internal structure of the Half Dome, where crosscutting relations in the field confirm that each deeper compositional cycle is younger than the overlying one [4]. Downward stacking of intrusive increments requires that water released by crystallization of younger increments ascends through older increments that already have crystallized before encountering wall rocks. Some of the water will likely move outward as well as upward, depending on permeability structure. A horizontal fluid conduit overlain by a flow barrier can force a significant amount of water to flow outward and form a wide hydrothermal aureole, as is seen around the Alta Stock, Utah [24,25]. However, even in such an example, it is likely that fluid is mainly transported upward toward the surface [13].

5. Fluid Transport Paths

Field and petrographic observations indicate that aqueous fluid released from crystallizing magma ascends via multiple paths (Figure 2). Perhaps the most obvious paths are fracture conduits which in a pluton are typically cooling joints where the infiltrating fluid leaves behind mineral precipitates to form hydrothermal veins (Figure 4a,b). Fractures undoubtedly are efficient fluid conduits and thus represent an important transport mode, but sealing of fractures by mineral precipitates gives them a limited lifetime unless deformation regenerates fracture permeability.

Focused fluid ascent also occurs via pipe-like conduits. In the Tuolumne Intrusive Suite, hydrothermal alteration is concentrated along pipes that range in diameter from a few decimeters to a meter or more (Figure 4c,d). The pipes are spatially associated with aplite and/or pegmatite dikes, in some instances confined to a dike and in others extending into adjacent granodiorite. The pipes are easily recognized in the field because they weather preferentially to form pits and even tunnels. Lines of pits along felsic dikes are common and thus, in locations where such dikes are abundant, pipe-like conduits are undoubtedly important fluid transport paths (Figure 4c,d). We do not yet know the nature of the porosity that governs formation of such hydrothermal pipes. We speculate that pipe formation involves open-system fluid–rock chemical reactions that reduce the volume of solid phases, increasing permeability where reactions take place and producing a positive feedback loop that further focuses fluid infiltration.

Not all fluid ascent through a pluton is focused along fractures and pipes, however. Hydrothermal veins are surrounded by haloes of altered rock that are visible in the field (Figure 4a,b). The haloes indicate that fluid penetrated into mesoscopically unfractured rock, apparently along microcracks and grain boundaries. Diffuse infiltration is locally reflected in the formation of endoskarn, that is, granitic rock in which primary texture persists but primary minerals have been extensively replaced by minerals such as albite, epidote, chlorite, and titanite (e.g., [13]). A key question, however, is whether grain-scale fluid infiltration is more pervasive but leaves behind a more subtle record than the bleached zones in Figure 3. Detailed petrography indicates that this is the case.

Thin rims or selvages of albite of near-end-member composition are commonly present along feldspar grain boundaries in granitic rocks (Figure 5). Rogers [26] attributed the albite to precipitation from an extremely fractionated late-stage intergranular melt. However, this origin is excluded by ternary feldspar phase equilibria which indicate that Na-rich feldspar precipitated from minimum-melt granite is anorthoclase rather than albite [27]. Phillips [28] attributed the albite to exsolution from primary igneous feldspars. However, the albite is found exclusively at contacts between plagioclase and K-feldspar or between K-feldspar grains. If exsolution were the process, albite should also be present at contacts between feldspar and other minerals such as quartz, but this is not observed. Moreover, perthite in which Na-rich and K-rich phases are intimately intermixed is the common product of K-feldspar exsolution; migration of exsolved albite to the external surface of a K-feldspar grain would be highly anomalous.

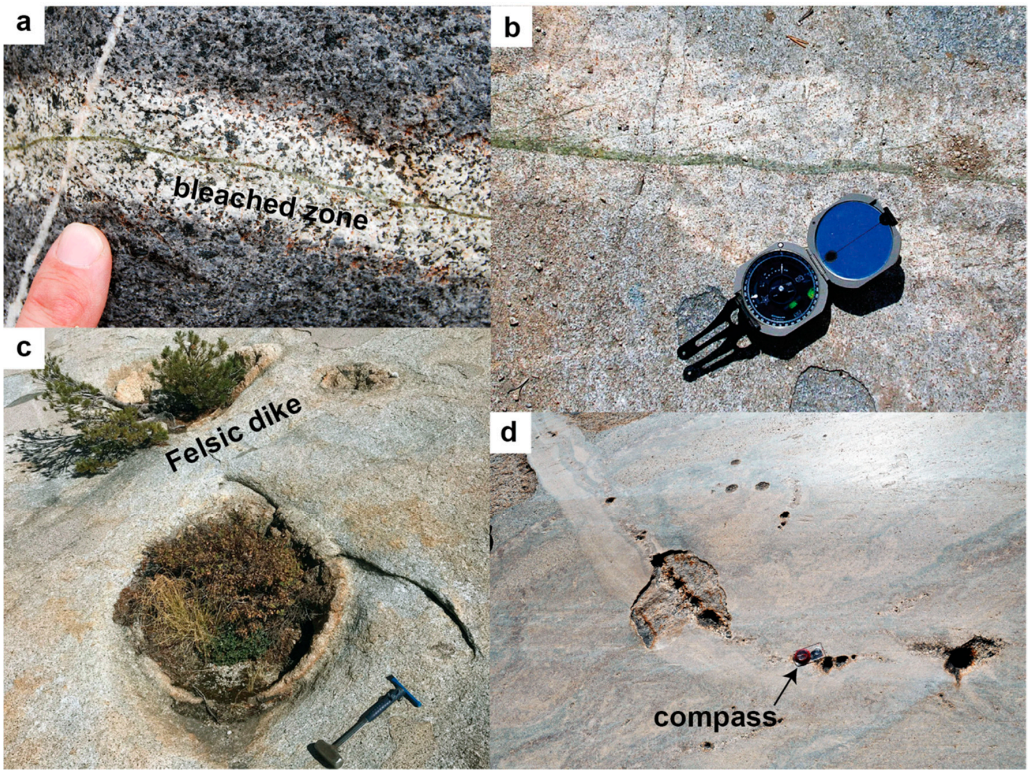

Figure 4. Field evidence of focused fluid transport in granitic plutons. (**a**) Fracture filled with hydrothermal epidote; diorite near Mack Lake, Sierra Nevada, California, USA. Note bleached zone around the vein. (**b**) Epidote-filled fracture network and surrounding bleached zone, Piute Creek, Sierra Nevada, California. (**c**) Pits weathered into large hydrothermal pipes, in and adjacent to felsic dike, Yosemite National Park, USA. (**d**) Line of pits weathered into hydrothermal pipes along contact of felsic dike, Yosemite National Park, USA (compass with 5 cm ring indicates scale).

The spatial distribution of albite thus is more consistent with O'Neil and Taylor's [29] inference that dissolution–precipitation is the likely mechanism for down-temperature re-equilibration of plutonic feldspars. Indeed, mineralogical, kinetic, isotopic, and microstructural evidence indicates that dissolution–precipitation is a widespread mechanism by which mineralogical changes take place in diverse geologic settings [30]. Localization of albite exclusively along feldspar–feldspar grain boundaries suggests interface-coupled precipitation of albite from a grain-boundary fluid (i.e., precipitation of albite occurred where a feldspar grain boundary provided a favorable nucleation surface). More speculatively, plagioclase-K-feldspar contacts may have been particularly favored for albite precipitation because albite-plagioclase and albite-K-feldspar contacts have lower surface energies than plagioclase-K-feldspar contacts [31].

Other microstructural observations from granitic rocks also support the importance of modification by interaction with a grain-boundary fluid. Cathodoluminescence (CL) imaging of feldspar in leucogranite from the Tuolumne Intrusive Suite in Yosemite (Figure 5b) reveals patchy and irregular internal zoning that is invisible in backscattered electron (BSE) imaging as well as in optical petrography. Unlike in quartz in which CL intensity variations largely reflect Ti content (e.g., [32]), the multiple trace-element activators that govern CL in feldspar are difficult to identify. However, the CL variations seen in Figure 5b,d indicate that different parts of a single crystal differ in their trace-element content and grew under different conditions. Such CL images are interpreted to record fracturing and healing of primary igneous grains that, if observed only optically or in BSE images, would likely be interpreted as unmodified after magmatic crystallization. Black spots on the BSE image in Figure 5a are micropores that probably reflect incomplete refilling of fractures [33]. Valley and Graham [32] presented similar CL images of quartz from granite on the Isle of Skye. Coupled with in situ oxygen isotopic analyses, these

textures demonstrate that " . . . the flow of hydrothermal fluids [that mediated dissolution–precipitation of quartz] was heterogeneous, anisotropic and crack controlled." Johnson et al. [34] imaged similar quartz textures in the Alta Granodiorite, Utah (Figure 5d), and also found that Ti contents of the quartz range down to values indicative of subsolidus crystallization.

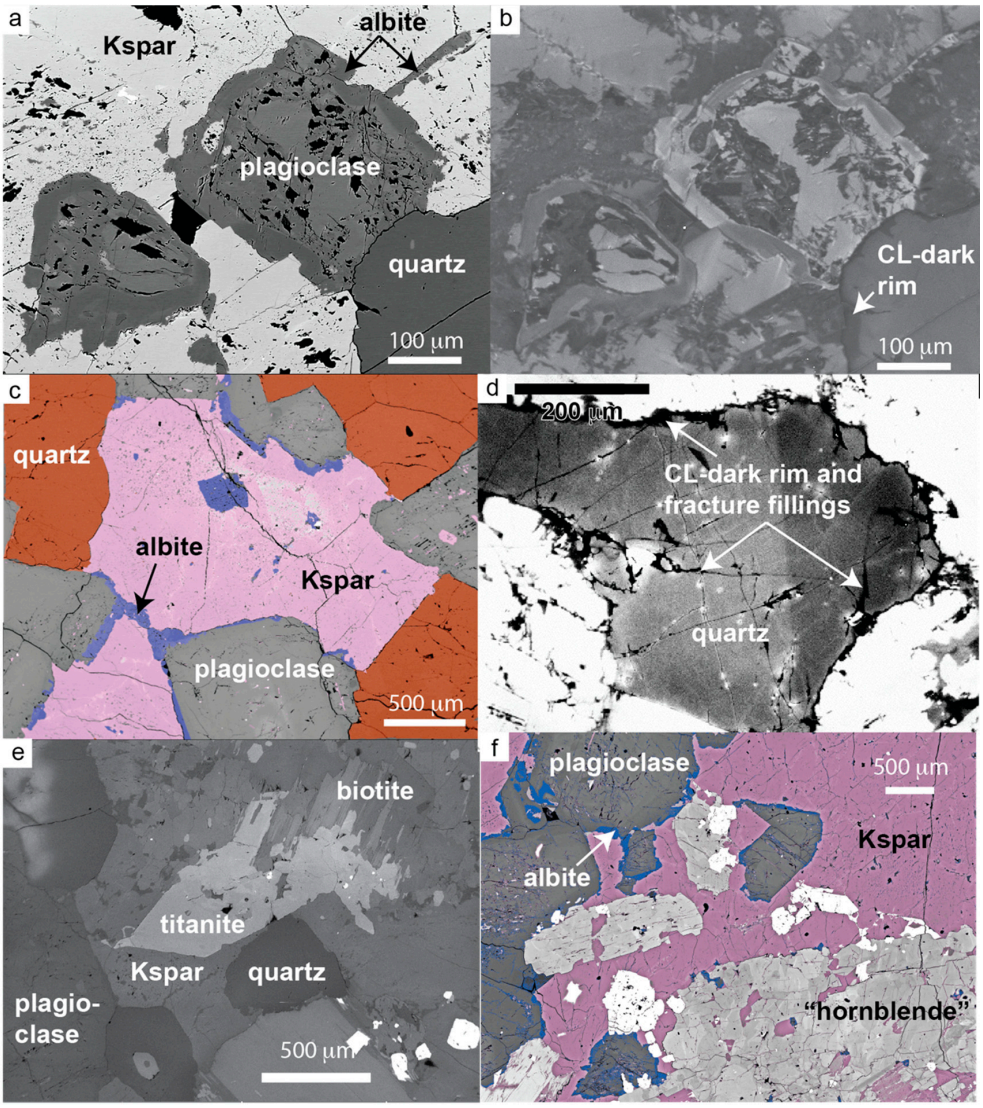

Figure 5. Backscattered electron (BSE) and cathodoluminescence (CL) images showing evidence of grain-scale modification by fluid infiltration. (**a**) BSE image of leucogranite, Tuolumne Intrusive Suite. BSE-dark albite selvages everywhere separate plagioclase from K-feldspar. (**b**) CL image of the same area as (**a**). Irregular patchy zoning of both feldspars reflects fracture, infiltration, and healing. The CL-dark (Ti-poor, low-temperature) rim on quartz reflects precipitation from grain-boundary fluid. (**c**) False-colored BSE image of Half Dome Granodiorite, Tuolumne Intrusive Suite, again showing albite along plagioclase-K-feldspar grain boundaries and locally within K-feldspar. (**d**) CL image of Alta Granodiorite, Utah [34]. CL-dark quartz rim and fracture fillings record precipitation from infiltrating fluid. (**e**) BSE image of Alta Granodiorite. Cores of euhedral titanite grains yield U-Pb dates of 36-31 Ma in agreement with U-Pb zircon dates from the same samples, whereas rims of euhedral grains and anhedral titanite intergrown with biotite give U-Pb dates as young as 23 Ma [13]. See text and reference [13] for further details. (**f**) False-colored BSE image of Half Dome Granodiorite. In addition to albite selvages, this image shows patchy zoning of "hornblende", which actually ranges in composition from hornblende to actinolite and records greenschist facies replacement (see text and ref. [35] for petrological details).

Textures seen in Figure 5a–d record interaction between minerals and fluids both at grain boundaries and in transgranular cracks. The micromechanics of grain-scale fractures are beyond the scope of this paper, but grain boundaries are mechanically favorable sites for cracks to form, both because they are weak and because differences in elastic properties across them result in stress concentrations. In rocks as inherently impermeable as granite, it is very likely that infiltration along grain boundaries was in cracks rather than in primary grain-boundary pore spaces of the sort seen in sandstone, for example. However, the grain-boundary stress concentrations also can produce transgranular fractures, particularly in minerals that contain cleavage planes. We therefore interpret the microstructures in Figure 5a–d to reflect crack-controlled fluid infiltration.

Textures, U-Pb dates, and Zr contents of titanite in the Alta and Little Cottonwood stocks reinforce the inference that the Alta Granodiorite was pervasively modified by an infiltrating aqueous fluid (Figure 5e; see [13] for full details). The cores of euhedral titanite grains yield in situ U-Pb dates that range from ca. 36 to 31 Ma, in agreement with U-Pb zircon dates from the same samples. Zirconium concentrations, determined simultaneously with U-Pb dates by split-stream analysis, indicate crystallization at approximately 650 °C (i.e., near the nominal granite solidus). In contrast, rims of these grains, as well as granular titanite that forms rims on Fe oxides and is intergrown with biotite, yield dates as young as 23 Ma and subsolidus Zr temperatures around 550 °C. We suggest that postmagmatic titanite in the Alta stock reflects reaction with infiltrating fluid released by crystallization of the underlying Little Cottonwood stock, which is a deeper part of the same magmatic system and grew incrementally through the time span recorded by titanite in the Alta stock [13].

Hornblende phenocrysts in the Half Dome Granodiorite commonly have been extensively modified by an infiltrating fluid under greenschist facies conditions [35]. Although euhedral and apparently intact when viewed in hand specimen, the patchy zoning seen in Figure 4f reflects a compositional range from actinolite to magmatic hornblende. The phenocrysts thus are pseudomorphs of the primary igneous amphibole. The phenocrysts host up to 50% inclusions of every mineral found in the rock including hydrous phases such as chlorite and epidote. Analyses of entire pseudomorphs by X-ray fluorescence yield a typical magmatic hornblende. Challener and Glazner [34] thus inferred replacement of primary magmatic hornblende that was isochemical except for the addition of water.

In summary, evidence from phase compositions and microstructures indicates pervasive subsolidus interaction with an aqueous fluid. In most cases, presently available evidence does not demand that that fluid was derived from crystallization of a deeper, younger part of the same pluton, although this is strongly suggested by data from the Alta and Little Cottonwood plutons [13].

6. Thermal Energy Carried by Escaping H_2O

In addition to facilitating dissolution–precipitation reactions and other forms of textural modification, upward-flowing H_2O carries a significant amount of thermal energy. As flow of vapor in fractures is orders of magnitude faster than heat conduction, this upward transfer of energy can have a significant effect on the thermal history of the crystallizing system.

The effect can be approximated using an enthalpy-composition (*H-X*) diagram constructed with thermodynamic data for water [36] and relevant minerals [37]. Construction of *H-X* diagrams was outlined by Ussler and Glazner [38]. Unlike familiar *T-X* diagrams, which involve the intensive parameter *T*, *H-X* diagrams use the extensive parameter *H* (specific enthalpy) and obey mass balance.

Figure 6 is a partial and partly schematic *H-X* diagram for the pseudobinary system haplogranite-H_2O at 200 MPa, constructed from these datasets relative to a standard state of 25 °C and 100 kPa (1 bar). Isotherms show *T* variation, and the eutectic, a point in a *T-X* diagram, is a triangle in the *H-X* rendering [38]. The diagram is based on data at and below the eutectic. Consequently, phase boundaries of the granite + melt and melt fields are purely schematic. The position of the melt apex of the eutectic is given by the water content of eutectic melt [39] and enthalpy calculations for water-saturated albite melt [40].

We assume a water-saturated granitic melt at 200 MPa with a liquidus at 950 °C and a solidus at 650 °C ([39], p. 52). Below the eutectic (which is the solidus), isotherms tie the solid quartz–feldspar

assemblage at 0 wt % H_2O with the vapor phase, which we idealize as pure H_2O. In our simplified model, the magma carries 5.5 wt % H_2O, releasing 5 wt % upon crystallization, and it reaches vapor saturation at the liquidus and releases H_2O linearly with temperature during crystallization; thus, half of the H_2O has been released as vapor at 800 °C.

If such a magma crystallizes to the solidus at 650 °C and retains its water as trapped vapor, the vapor phase has a specific enthalpy H of 2830 J/g; the solid assemblage has H = 750 J/g. This large difference results from the higher heat capacity of H_2O and its large enthalpy of vaporization. If this vapor escapes via fractures and invades cooler rock above without cooling, it carries a significant amount of thermal energy into the cooler rock volume (for simplicity we assume that depth, and thus pressure, differences are small so that we ignore them in the calculations). For example, in the case of rapid transport, idealized as an adiabatic case, if this vapor thermally equilibrates with an equal mass of 300 °C rock around the fractures, the temperature of the equilibrated volume will be about 570 °C (Figure 6, point A). If vapor from crystallizing magma at 800 °C invades and equilibrates with rock at 500 °C, it will induce melting if the mass fraction of H_2O is approximately 0.25 or greater (point B).

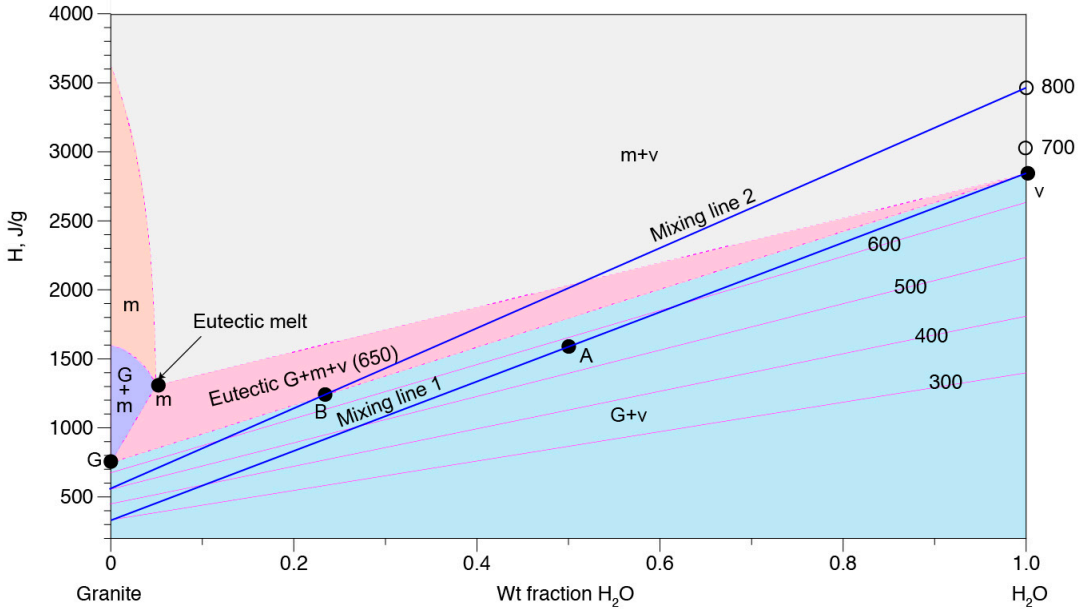

Figure 6. Schematic enthalpy-composition (*H-X*) diagram for the system haplogranite–H_2O. H_2O has a much higher specific enthalpy than minerals, and so it carries a significant amount of heat (see text). At and below the eutectic triangle, the diagram is based on thermodynamic data, but phase boundaries on the left side are just schematic. Diagonal magenta lines are isotherms. For clarity, isotherms are not shown above the eutectic. The open circles on the right-hand vertical axis locate the enthalpy of pure H_2O at 700° and 800 °C; the corresponding isotherms extend from the open circles in orientations subparallel to the lower-temperature isotherms. Blue lines are mixing lines between H_2O and the solid quartz–feldspar assemblage. Note that the 800 °C mixing line crosses the solidus (i.e., a water-rock ratio > ca. 0.33 at this temperature) will cause remelting.

7. Other Evidence of Late-Stage Textural Modification

A number of studies report evidence of late- to postmagmatic modification of plutonic minerals and textures that is not demonstrably tied to fluid infiltration, but it is probable that pore fluid was involved. Diffusion modeling of Ti zoning in quartz from the Tuolumne Intrusive Suite led Ackerson et al. [41] to conclude that up to 80% of the quartz in these granitic rocks crystallized at temperatures 100–200 °C below the nominal solidus. Because the modal proportion of quartz does not differ from its magmatic abundance, this demands recrystallization of the primary quartz. Such recrystallization might not have

happened in the presence of an aqueous fluid, but dissolution–reprecipitation in a grain-boundary fluid probably is the most feasible mechanism.

Higgins [42] and Johnson and Glazner [43,44] presented textural and mineralogical evidence that K-feldspar megacrysts in granitic rocks reflect late-stage textural coarsening in which smaller crystals are consumed and their constituents are transported to feed the growth of megacrysts. The precise mechanism is uncertain, as is the presence or absence of a melt phase when it happened. Higgins [42] proposed Ostwald ripening, that is, coarsening driven by minimization of surface free energy, but this is unlikely if recrystallization was driven only by surface free energy [45,46]. However, the assertion that crystal coarsening does not happen in coarsely crystalline materials because Ostwald ripening is ineffective (e.g., [47,48]) is clearly contradicted by diverse studies in materials science including petrology (e.g., [49–52]).

Textural coarsening in plutonic rocks likely results from dissolution–precipitation caused by fluctuating temperature, fluid infiltration, and concomitant mineral reactions. The consistently K-rich composition of the megacrysts (typically $Or_{85\text{-}90}$ from core to rim [43,44]) indicates equilibration with plagioclase at ca. 400 °C, far below the nominal solidus. The megacrysts also are extremely Ca-poor (ca. $An_{0.1}$), which not only corroborates a low equilibration temperature but also excludes diffusive exchange as an equilibration mechanism owing to the low diffusivity of Ca in feldspar [44]. The change of magmatic alkali feldspar to its present low-temperature composition need not be directly linked to textural coarsening, but this mineral reaction has invariably affected K-feldspar megacrysts and it would contribute energy to drive the textural change. The common presence of overgrown corrosion surfaces inside the megacrysts indicates that megacryst growth was not monotonic and suggests a specific process. Primary magmatic K-feldspar grains were episodically corroded by an increase in temperature, infiltration of a fluid, or both. The larger surviving grains regrow preferentially because they provide nucleation surfaces onto which components in the fluid can crystallize. Repeated fluctuations ultimately lead to the demise of small grains, a process that is clearly observed in real time in thermal cycling experiments [49–52]. Pulses of both heat and fluids released by crystallization of later increments into already-crystallized granite thus are strong candidates for facilitating both textural coarsening and modification of primary igneous feldspar compositions.

8. Summary

Subduction-related magmas transport and release large quantities of water into the crust. Water released by crystallizing magma probably escapes along multiple paths through previously crystallized plutonic rock. It is difficult to quantify how much of the water follows each path, but it is likely that a large fraction is channeled along fractures and pipes. However, pervasive infiltration of aqueous fluid along grain boundaries and microfractures commonly has significantly modified primary mineral compositions and textures. We suggest that the infiltrating fluid was derived from crystallization of younger, deeper magmatic increments added to the growing pluton. This suggestion is clearly speculative; more evidence is needed to test whether the grain-boundary fluid was derived from cogenetic magma.

Fluid release from crystallizing magma does not affect the temperature of the magma but the fluid advects a large fraction of the magma's energy into adjacent already-solidified granite. This implies that the sawtooth postsolidus thermal histories predicted for early intrusive increments by conductive incremental-growth thermal models (e.g., [15]) substantially underestimate the actual amplitude of the thermal fluctuations. In some instances, infiltration of magmatic fluid may produce not only mineral reactions and textural modification but also remelting of previously solidified portions of the pluton. Remelting of already solidified granite by this mechanism would be difficult to conclusively demonstrate because the result will be a granitic pore melt in a matrix of granite; therefore, cooling will merely redeposit quartz and feldspars on crystals that survived remelting. The result is likely to be textural modifications that would be difficult to distinguish from subsolidus textural modifications.

The sparseness of mappable internal contacts in plutons is a major reason that the incremental growth of plutons over million-year time scales was not recognized until the development of

high-precision geochronology. We suggest that an important reason that increment contacts are rarely observable in the field is extensive postemplacement textural modification. Modification is a practically inevitable consequence of incremental growth because much, if not all, of the modification is caused by pulses of water and heat released by magmatic crystallization entering already-crystallized portions of the pluton.

Author Contributions: Conceptualization, J.M.B., A.F.G., M.A.S., D.S.C.; methodology, J.M.B., A.F.G., M.A.S., D.S.C.; formal analysis, A.F.G., M.A.S.; investigation, J.M.B., A.F.G., M.A.S.; resources, J.M.B., A.F.G., M.A.S.; data curation, A.F.G., M.A.S.; writing—original draft preparation, J.M.B.; writing—review and editing, A.F.G., M.A.S., D.S.C.; visualization, J.M.B., A.F.G., M.A.S.; project administration, J.M.B., A.F.G., M.A.S., D.S.C.; funding acquisition, J.M.B., A.F.G., M.A.S., D.S.C. All authors have read and agreed to the published version of the manuscript.

Funding: This research was funded by the U.S. National Science Foundation through grant numbers EAR-0538094 and EAR-1853496 to J.B.; grant number EAR-1250505 to A.G.; grant number EAR-0538129 to A.G. and D.C.; and grant number EAR-1853496 to M.S. A.G. also gratefully acknowledges support from the Mary Lily Kenan Flagler Bingham Professorship.

Acknowledgments: Discussions with Ryan D. Mills and John R. Bowman contributed to development of the ideas presented in this paper. Input from two anonymous reviewers helped us to improve the clarity of the paper. U.S. National Park Service personnel, especially Greg Stock, Jan van Wagtendonk, and Peggy Moore, have been supportive and helpful to our field studies in Yosemite. John Bowman provided the CL image from the Alta Granodiorite in Figure 4d.

Conflicts of Interest: The authors declare no conflict of interest.

References

1. Carmichael, I.S.E. The andesite aqueduct: Perspectives on the evolution of intermediate magmatism in west-central (105–99°W) Mexico. *Contr. Miner. Petrol.* **2002**, *143*, 641–663. [CrossRef]
2. Coleman, D.S.; Gray, W.; Glazner, A.F. Rethinking the emplacement and evolution of zoned plutons: Geochronologic evidence for the incremental assembly of the Tuolumne Intrusive Suite, California. *Geology* **2004**, *32*, 433–436. [CrossRef]
3. Michel, J.; Baumgartner, L.; Putlitz, B.; Schaltegger, U.; Ovtcharova, M. Incremental growth of the Patagonian Torres del Paine laccolith over 90 k.y. *Geology* **2008**, *36*, 459–462. [CrossRef]
4. Coleman, D.S.; Bartley, J.M.; Glazner, A.F.; Pardue, M.J. Is chemical zonation in plutonic rocks driven by changes in source magma composition or shallow-crustal differentiation? *Geosphere* **2012**, *8*, 1568–1587. [CrossRef]
5. Bartley, J.M.; Glazner, A.F.; Coleman, D.S. Dike intrusion and deformation during growth of the Half Dome pluton, Yosemite National Park, California. *Geosphere* **2018**, *14*, 1–15. [CrossRef]
6. Sisson, T.W.; Layne, G.D. H_2O in basalt and basaltic andesite glass inclusions from four subduction-related volcanoes. *Earth Plan. Sci. Lett.* **1993**, *117*, 619–635. [CrossRef]
7. Wallace, P.J. Volatiles in subduction zones magmas: Concentrations and fluxes based on melt inclusion and volcanic gas data. *J. Volc. Geotherm. Res.* **2005**, *140*, 217–240. [CrossRef]
8. Metrich, N.; Wallace, P.J.; Putirka, K.D.; Frank, J., III. Volatile abundances in basaltic magmas and their degassing paths tracked by melt inclusions. *Rev. Miner. Geochem.* **2008**, *69*, 363–402. [CrossRef]
9. Plank, T.; Kelley, K.A.; Zimmer, M.M.; Hauri, E.H.; Wallace, P.J. Why do mafic arc magmas contain ~4 wt % water on average? *Earth Plan. Sci. Lett.* **2013**, *364*, 168–179. [CrossRef]
10. Grove, T.; Parman, S.; Bowring, S.; Price, R.; Baker, M. The role of an H_2O-rich fluid component in the generation of primitive basaltic andesites and andesites from the Mt. Shasta region, N California. *Contr. Miner. Petrol.* **2002**, *143*, 641–663. [CrossRef]
11. Laumonier, M.; Gaillard, F.; Muir, D.; Blundy, J.; Unsworth, M. Giant magmatic water reservoirs at mid-crustal depth inferred from electrical conductivity and growth of the continental crust. *Earth Plan. Sci. Lett.* **2016**, *457*, 173–180. [CrossRef]
12. Matzel, J.E.P.; Bowring, S.A.; Miller, R.B. Time scales of pluton construction at differing crustal levels; examples from the Mount Stuart and Tenpeak Intrusions, north Cascades, Washington. *Geol. Soc. Am. Bull.* **2006**, *118*, 1412–1430. [CrossRef]

13. Stearns, M.A.; Bartley, J.M.; Bowman, J.R.; Forster, C.W.; Beno, C.J.; Riddle, D.D.; Callis, S.J.; Udy, N.D. Simultaneous magmatic and hydrothermal regimes recorded by multiphase U-Pb petrochronology, Alta-Little Cottonwood stocks, Utah, USA. *Geosciences* **2020**, *10*, 129. [CrossRef]
14. Glazner, A.F.; Bartley, J.M.; Coleman, D.S.; Gray, W.; Taylor, R.Z. Are plutons assembled over millions of years by amalgamation of small magma chambers? *GSA Today* **2004**, *14*, 4–11. [CrossRef]
15. Annen, C.; Scaillet, B.; Sparks, R.S.J. Thermal constraints on the emplacement rate of a large intrusive complex: The Manaslu Leucogranite, Nepal Himalaya. *J. Petrol.* **2006**, *47*, 71–95. [CrossRef]
16. Bartley, J.M.; Coleman, D.S.; Glazner, A.F. Incremental emplacement of plutons by magmatic crack-seal. *Trans. R. Soc. Edinb.* **2006**, *97*, 383–396. [CrossRef]
17. Pitcher, W.S.; Berger, A.R. *The Geology of Donegal: A Study of Granite Emplacement and Unroofing*; Wiley-Interscience: New York, NY, USA, 1972.
18. Mahan, K.H.; Bartley, J.M.; Coleman, D.S.; Glazner, A.F.; Carl, B.S. Sheeted intrusion of the synkinematic McDoogle pluton, Sierra Nevada, California. *Geol. Soc. Am. Bull.* **2003**, *115*, 1570–1582. [CrossRef]
19. Leuthold, J.; Muentener, O.; Baumgartner, L.P.; Putlitz, B.; Ovtcharova, M.; Schaltegger, U. Time resolved construction of a bimodal laccolith (Torres del Paine, Patagonia). *Earth Plan. Sci. Lett.* **2012**, *325*, 85–92. [CrossRef]
20. Davis, J.W.; Coleman, D.S.; Gracely, J.T.; Gaschnig, R.; Stearns, M. Magma accumulation rates and thermal histories of plutons of the Sierra Nevada batholith, CA. *Contr. Miner. Petrol.* **2012**, *163*, 449–465. [CrossRef]
21. Horsman, E.; Tikoff, B.; Morgan, S. Emplacement-related fabric and multiple sheets in the Maiden Creek sill, Henry Mountains, Utah, USA. *J. Struct. Geol.* **2005**, *27*, 1426–1444. [CrossRef]
22. Farina, F.; Dini, A.; Innocenti, F.; Rocchi, S.; Westerman, D.S. Rapid incremental assembly of the Monte Capanne pluton (Elba Island, Tuscany) by downward stacking of magma sheets. *Geol. Soc. Am. Bull.* **2010**, *122*, 1463–1479. [CrossRef]
23. Gaynor, S.P.; Coleman, D.S.; Rosera, J.M.; Tappa, M.J. Geochronology of a Bouguer gravity low. *J. Geophys. Res.* **2018**, *124*, 1–12. [CrossRef]
24. Cook, S.J.; Bowman, J.R. Contact metamorphism surrounding the Alta stock; thermal constraints and evidence of advective heat transport from calcite + dolomite geothermometry. *Am. Min.* **1994**, *79*, 513–525.
25. Cook, S.J.; Bowman, J.R.; Forster, C.B. Contact metamorphism surrounding the Alta Stock; finite element model simulation of heat- and $^{18}O/^{16}O$ mass-transport during prograde metamorphism. *Am. J. Sci.* **1997**, *297*, 1–55. [CrossRef]
26. Rogers, J.J.W. Origin of albite in granitic rocks. *Am. J. Sci.* **1961**, *259*, 186–193. [CrossRef]
27. Carmichael, I.S.E. The crystallization of feldspar in volcanic acid liquids. *J. Geol. Soc. Lond.* **1963**, *119*, 95–130. [CrossRef]
28. Phillips, E.R. Myrmekite and albite in some granites of the New England Batholith, New South Wales. *J. Geol. Soc. Austr.* **1964**, *11*, 49–60. [CrossRef]
29. O'Neil, J.R.; Taylor, H.P.J. The oxygen isotope and cation exchange. *Am. Min.* **1967**, *52*, 1414–1437.
30. Putnis, A.; John, T. Replacement processes in the Earth's Crust. *Elements* **2010**, *6*, 159–164. [CrossRef]
31. Glazner, A.F. K-feldspar and cooties; or why K-feldspar likes to grow into big crystals. In Proceedings of the GSA Annual Meeting, Phoenix, AZ, USA, 22–25 September 2019.
32. Valley, J.W.; Graham, C.M. Ion microprobe analysis of oxygen isotope ratios in quartz from Skye granite; healed micro-cracks, fluid flow, and hydrothermal exchange. *Contr. Miner. Petrol.* **1996**, *124*, 225–234. [CrossRef]
33. Glazner, A.F.; Bartley, J.M.; Coleman, D.S.; Lindgren, K. Aplite diking and infiltration: A differentiation mechanism restricted to plutonic rocks. *Cont. Min. Petrol.* **2020**, *175*, 37. [CrossRef]
34. Johnson, B.W.; Bowman, J.R.; Nash, B.P.; Valley, J.W.; Bartley, J.M. Oxygen isotope, TitaniQ, and cathodoluminescence analyses of the Alta stock, UT: Preliminary insights into pluton assembly. *Geol. Soc. Am. Abstr.* **2009**, *41*, 43.
35. Challener, S.C.; Glazner, A.F. Igneous or metamorphic? Hornblende phenocrysts as greenschist facies reaction cells in the Half Dome Granodiorite, California. *Am. Min.* **2017**, *102*, 436–444. [CrossRef]
36. Burnham, C.W.; Holloway, J.R.; Davis, N.F. *Thermodynamic Properties of Water to 1000 °C and 10,000 Bars*; Geological Society of America: Boulder, CO, USA, 1969.

37. Robie, R.A.; Hemingway, B.S.; Fisher, J. Thermodynamic properties of Minerals and Related Substances at 298.15 K and 1 Bar (105 Pascals) Pressure and at Higher Temperatures. 1978. Available online: https://pubs.er.usgs.gov/publication/b2131 (accessed on 10 April 2020).
38. Ussler, W., III; Glazner, A.F. Graphical analysis of enthalpy-composition relationships in mixed magmas. *J. Volc. Geotherm. Res.* **1992**, *51*, 23–40. [CrossRef]
39. Johannes, W.; Holtz, F. *Petrogenesis and Experimental Petrology of Granitic Rocks*; Springer: New York, NY, USA, 1996.
40. Glazner, A.F. The ascent of water-rich magma and decompression heating: A thermodynamic analysis. *Am. Min.* **2019**, *104*, 890–896. [CrossRef]
41. Ackerson, M.R.; Mysen, B.O.; Tailby, N.D.; Watson, E.B. Low-temperature crystallization of granites and the implications for crystal magmatism. *Nature* **2018**, *559*, 94–97. [CrossRef] [PubMed]
42. Higgins, M.D. Origin of megacrysts in granitoids by textural coarsening; a crystal size distribution (CSD) study of microcline in the Cathedral Peak Granodiorite, Sierra Nevada, California. *Geol. Soc. Spec. Pubs.* **1999**, *168*, 207–219. [CrossRef]
43. Johnson, B.R.; Glazner, A.F. Formation of K-feldspar megacrysts in granodioritic plutons by thermal cycling and late-stage textural coarsening. *Contr. Miner. Petrol.* **2010**, *159*, 599–619. [CrossRef]
44. Glazner, A.F.; Johnson, B.R. Late crystallization of K-feldspar and the paradox of megacrystic granites. *Contr. Min. Petrol.* **2013**, *166*, 777–799. [CrossRef]
45. Cabane, H.; Laporte, D.; Provost, A. Experimental investigation of the kinetics of Ostwald ripening of quartz in silicic melts. *Contrib. Miner. Petrol.* **2001**, *142*, 361–373. [CrossRef]
46. Cabane, H.; Laporte, D.; Provost, A. An experimental study of Ostwald ripening of olivine and plagioclase in silicate melts; implications for the growth and size of crystals in magmas. *Contrib. Miner. Petrol.* **2005**, *150*, 37–53. [CrossRef]
47. Holness, M.B.; Vernon, R.H. The influence of interfacial energies on igneous microstructures. In *Layered Intrusions*; Charlier, B., Namur, O., Latypov, R., Tegner, C., Eds.; Springer: Dordrecht, The Netherlands, 2015; pp. 183–227.
48. Gualda, G.A.R. On the origin of alkali feldspar megacrysts in granitoids: The case against textural coarsening. *Contr. Miner. Petrol.* **2019**, *174*, 88. [CrossRef]
49. Mills, R.D.; Glazner, A.F. Experimental study on the effects of temperature cycling on coarsening of plagioclase and olivine in an alkali basalt. *Contrib. Miner. Petrol.* **2013**, *166*, 97–111. [CrossRef]
50. Erdmann, M.; Koepke, J. Experimental temperature cycling as a powerful tool to enlarge melt pools and crystals at magma storage conditions. *Am. Miner.* **2016**, *101*, 960–969. [CrossRef]
51. Donhowe, D.P.; Hartel, R.W. Recrystallization of ice cream during controlled accelerated storage. *Int. Dairy J.* **1996**, *6*, 1191–1208. [CrossRef]
52. Mills, R.D.; Ratner, J.J.; Glazner, A.F.; Mills, R.D. Experimental evidence for crystal coarsening and fabric development during temperature cycling. *Geology* **2011**, *39*, 1139–1142. [CrossRef]